Aluminium and iron record for the last 28 kyr derived from the Antarctic EDC96 ice core using new CFA methods

Rita TRAVERSI,[1] Carlo BARBANTE,[2,3] Vania GASPARI,[2] Ilaria FATTORI,[1]
Ombretta LARGIUNI,[1] Lorenzo MAGALDI,[1] Roberto UDISTI[1]

[1] Chemistry Department – Analytical Chemistry, Scientific Pole, University of Florence, Via della Lastruccia 3,
I-50019 Sesto Fiorentino (Florence), Italy
E-mail: rita.traversi@unifi.it
[2] Department of Environmental Sciences, University of Venice, Dorsoduro 2137, I-30123, Italy
[3] Institute for the Dynamics of Environmental Processes (CNR), University of Venice, Dorsoduro 2137, I-30123, Italy

ABSTRACT. Spectrofluorimetric and spectrophotometric continuous flow analysis (CFA) methods were developed and applied to the determination of aluminium and iron in EPICA Dome C (East Antarctica) ice-core samples (6–585 m depth). The methods are able to measure the fraction of Al and Fe which can be detected once the sample is filtered on a 5.0 μm membrane and acidified to pH 2. Both the methods present high sensitivity (detection limit of $10\,ng\,L^{-1}$ for Al and $50\,ng\,L^{-1}$ for Fe) and reproducibility (5% at sub-ppb level). The Fe and Al profiles show sharp decreases in concentrations in the last glacial/interglacial transition, reflecting the decreasing dust aerosol load. The two elements show a different pattern during the Antarctic Cold Reversal (ACR) climatic change, with high iron concentrations (similar to the glacial period) and low but increasing Al content during the ACR minimum. In order to interpret the Al and Fe data obtained by CFA, a comparison with Al and Fe composition, as measured by inductively coupled plasma sector field mass spectrometry (ICP-SFMS), was performed for Holocene, ACR and glacial periods. The percentage of CFA-Al with respect to ICP-SFMS-Al in the three periods shows a lower variability than CFA-Fe (3% in the glacial period and 64% in the ACR). This pattern may be explained by the different dominant iron sources in the different climatic periods. During the Last Glacial Maximum, Fe is proposed to arise mainly from insoluble continental dust, while a variety of ocean-recycled Fe, mainly distributed in fine particles and as more soluble species, shows a higher contribution in the ACR and, to a lesser extent, in the Holocene.

INTRODUCTION

Extremely low concentrations of dissolved iron in surface waters of remote ocean regions (Johnson and others, 1997) are believed to play a key role in controlling biological productivity in these regions, despite the abundance of major nutrients (Martin and Fitzwater, 1988). These high-nutrient low-chlorophyll (HNLC) regions, as they are usually referred to, are found in several oceanic regions with limited aeolian deposition such as the Southern Ocean. Iron limitation may influence many phytoplankton physiological processes, including photosynthetic energy conversion efficiency (e.g. Greene and others, 1994), NO_3^- assimilation (e.g. Raven, 1990) and chlorophyll synthesis (Chereskin and Castelfranco, 1982).

The so-called 'iron hypothesis', proposed by Martin (1990), was a major advance in this field of research; it linked changes in iron supply to the ocean with variations in primary production rates and with subsequent present and past uptake of carbon in HNLC waters.

Redox reactions, complexation, adsorption and precipitation processes control the concentration of iron in natural waters. Dissolved iron can exist in two oxidation states, Fe(II) and Fe(III), free or complexed with inorganic or organic ligands. The availability of iron in ocean waters is mostly limited by the solubility of Fe(III) (Johnson and others, 1997). Reduction of Fe(III) to Fe(II), with subsequent reoxidation to Fe(III) by photochemical or other processes, possibly increases the bio-availability of colloidal iron to phytoplank-

ton (Finden and others, 1984; Wells and others, 1991). Therefore, the determination of both soluble Fe(III) and Fe(II) species is relevant in assessing the Fe available fraction for biological processes.

Aluminium, the third most abundant element in the Earth's crust (8.2%), occurs in a large variety of oxide minerals and, together with silicon, forms aluminosilicate clays and soils. Nevertheless, oceanic Al concentrations are extremely low and its distribution in surface waters can help identify the source and magnitude of continentally derived dust contributions to the ocean (Measures, 1999).

Mineral dust has been identified as an important primary aerosol constituent (Andreae, 1996). At global scales, dust is a major source of minerals (Duce, 1995) and associated nutrients (Prospero, 1996) to the global ocean.

Aluminium in environmental matrices occurs as both 'dissolved' and particulate species. The former includes aluminium in solution and in the colloidal form, mainly consisting of hydroxy compounds of the metal. The particulate species mainly consists of aluminosilicate minerals of detrital and terrigeneous origin (Mánuel-Vez and others, 1997).

Fe and Al temporal profiles from polar ice cores can provide information on past atmospheric compositions linked to palaeoclimatic and palaeoenvironmental conditions.

Few Al measurements have been carried out on polar ice cores, although De Angelis and others (1984, 1987) and Legrand and others (1988) used Al as a specific crustal
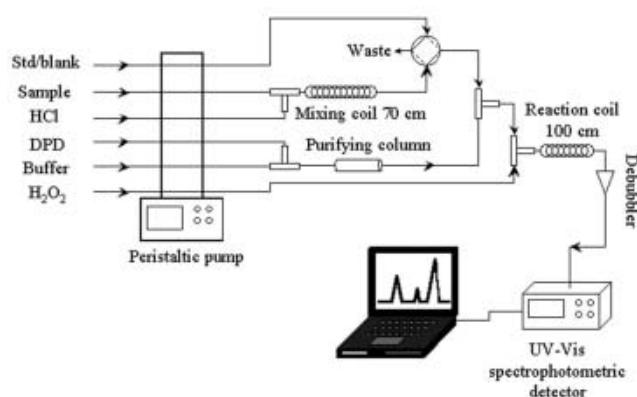
Fig. 1. Schematic representation of the CFA method for Fe determination.

Fig. 2. Schematic representation of the CFA method for Al determination.

marker to evaluate the terrestrial contribution to ionic compounds in the last glacial/interglacial cycle from analysis of the Vostok (East Antarctica) ice core. As for iron, although it is strictly related to crustal sources and is a potential tracer of dust depositions, its key role in marine biocycles suggests that this element, especially its bio-available fraction, can provide information on ocean biogenic productivity.
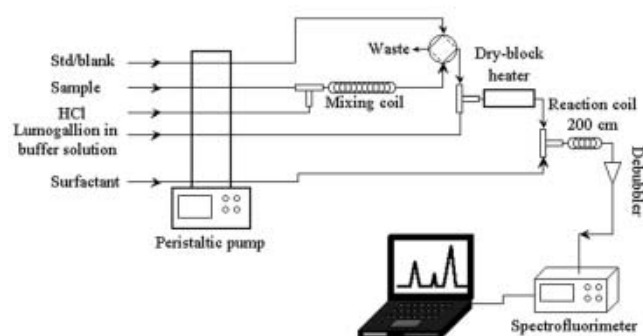
For this purpose, two flow-analysis systems for Fe and Al determination were set up and used to analyze samples from the EPICA Dome C (EDC96) (East Antarctica) ice core; data were used to identify variations in these elements during the last glacial/interglacial transition and to infer palaeoclimatic conditions.

EXPERIMENTAL METHODS

The analytical method for measuring Fe is based on a continuous flow analysis (CFA) spectrophotometric determination and takes advantage of the ability of the Fe(III) ion to oxidize the N,N'-dimethyl-p-phenylenediamine (DPD) to a semiquinonic form (DPDQ) in the presence of H_2O_2.

Measurements were performed at 514 nm wavelength, where DPDQ shows a maximum of absorption (Hirayama and Unohara, 1988; Measures and others, 1995).

The reaction develops in a slightly acidic medium (pH = 5.2) and proceeds very slowly in the absence of Fe(III), which acts as a catalyst by electronic transfer. The catalytic reaction involving Fe(III) occurs as follows: Fe(III) oxidizes the DPD, quantitatively producing DPDQ and reducing

itself to Fe(II); H_2O_2 regenerates Fe(III) by Fe(II) oxidation, concluding the redox cycle. In this way, the Fe(II) already present in the examined solution is oxidized to Fe(III) by H_2O_2, allowing the determination of the Fe(II) and Fe(III) species available in the measurement conditions.

In order to minimize the reagent blank values, a purifying column containing a chelating resin (IC Alltech) was inserted in the reagent line before mixing with the sample due to the presence of iron impurities in the DPD and buffer solutions.

Figure 1 shows the instrumentation for Fe determination; basic information on reagents and flows is reported in Table 1.

The determination of Al is accomplished by a CFA spectrofluorimetric method based on the formation of a fluorescent compound between aluminium and the lumo-gallion ligand (4-chloro-6-[(2,4-dihydroxyphenyl)azo]-1-hydroxybenzene-2sulfonic acid; Nishikawa and others, 1967). This reagent has already been employed by several authors (e.g. Resing and Measures, 1994), and the kinetics of the formation reaction for the Al-lumogallion complex has also been investigated (Sutheimer and Cabaniss, 1997).

Figure 2 shows a flow chart of the system. The complex-ation reaction occurs at 70°C, and fluorescence is preserved by adding a non-ionic surfactant (Brij-35). Measurements were performed at the excitation and emission wavelengths of 484 and 552 nm, respectively. Reagent compositions, concentrations and flow are reported in Table 2.

Fluorescence detection with an Al-lumogallion complex was demonstrated to quantitatively determine all forms of dissolved aluminium except polymers, making the method useful as a speciation procedure for determining free and complexed (organic and inorganic) forms of aluminium (Sutheimer and Cabaniss, 1995).

Table 1. Composition, concentration and flow of the reagents used for Fe determination. Standard solutions for calibration curve were prepared daily by dilution of the Merck certified standard

Reagents	Composition	Flow mL min^{-1}	Concentration
Blank	Ultrapure MilliQ water	0.57	
Standard	Obtained from Merck certified standard: Fe 1.00 g L^{-1} in HNO$_3$ 0.5 M	0.57	0.1 ÷ 5 µg L^{-1}
Reducing agent	N,N-dimethyl-p-phenylendiamine (DPD)	0.15	0.09 M
Oxidizing agent	H$_2$O$_2$ suprapur	0.24	5% w/w
Buffer	CH$_3$COONa/CH$_3$COOH suprapur	0.71	0.25 M
Sample acidifier	HCl suprapur	0.06	0.32 M

Table 2. Composition, concentration and flow of the reagents used for Al determination. Standard solutions for calibration curve were prepared daily by dilution of the Merck certified standard

Reagents	Composition	Flow mL min^{-1}	Concentration
Blank	Ultrapure MilliQ water	0.57	
Standard	obtained from Merck certified standard: Al 1.00 g L^{-1} in HNO$_3$ 0.5 M	0.57	0.1 ÷ 2 µg L^{-1}
Lumogallion in acetic buffer	4-chloro-6-[(2,4-dihydroxy-phenyl)azo]-1-hydroxybenzene-2-sulfonic acid	0.71	0.09 M
Buffer	CH$_3$COONa/CH$_3$COOH suprapur	0.71	0.25 M
Surfactant	Brij-35	0.08	6% (w/w)
Sample acidifier	HCl suprapur	0.06	0.32 M

Analytical parameters were optimized in both methods in order to enhance their sensitivity and reproducibility which were sufficient to measure low Al and Fe concentration levels present in EDC96 samples without preconcentration. Reproducibility, linearity ranges and detection limits for the adopted analytical methods are reported in Table 3.

For both determinations, sample treatment, preparation and storage of reagents were carried out in a clean room under a class 100 laminar-flow hood to limit possible contamination.

Since the CFA methods are able to determine the free or, in some cases, labile complexed form of the dissolved metal, which is thought to be strictly dependent on particle size distribution, the samples were filtered on a 5.0 µm membrane and then acidified (pH 2 with HCl) on-line in order to select the desired size range and to make as much metal as possible available for measurement.

Fe and Al CFA measurements were compared with metal content determined at the Department of Environmental Sciences, University of Venice, by inductively coupled plasma sector field mass spectrometry (ICP-SFMS) using a Finnigan MAT Element instrument (Barbante and others, 1997, 1999; Planchon and others, 2001). For most samples, a Teflon PFA self-aspirating nebulizer (Elemental Scientific, Omaha, NE, USA) was used in free-running mode. Working conditions and measurement parameters are described in detail in Planchon and others (2001). Special attention was paid to possible interference (Planchon and others, 2001). Detection limits range from 5 ng L^{-1} for Fe to 15 ng L^{-1} for Al, with an uptake rate of 60–80 µL of sample per minute. Most analyses were performed directly without preconcentration.

The analytical methods presented were developed to perform continuous analysis of polar ice cores with an ice-melting system (Röthlisberger and others, 2000), but up to now they have only been tested on about 1000 discontinuous samples from the EPICA Dome C ice core in the 6–585 m depth range covering the last 28 kyr.

Table 3. Performance of the new CFA methods for Fe and Al determination

	Fe	Al
Relative standard deviation (calculated on a 0.5 µg L^{-1} std solution)	5%	5%
Linearity range (µg L^{-1})	0–50	0–200
Detection limit (µg L^{-1})	0.05	0.01

The samples were assigned to the Florence laboratory for ion chromatographic (IC) analysis in the framework of the EPICA (European Project for Ice Coring in Antarctica) Chemistry Consortium. The bag strips were decontaminated by mechanical removal of the external layer using a microtome blade and subsampled with an average resolution of 5 cm. Decontamination and subsampling operations were performed in a cold room under a class 100 laminar-flow hood. Fe and Al measurements were carried out on the refrozen subsample volume left after IC analysis.

DATA DISCUSSION

The concentration vs depth profiles for Fe and Al are reported in Figure 3 where the dots represent the average (usually ten values) of a 55 cm long ice-core section (bag) and the vertical bars represent the standard deviation related to each bag. On the top of the plot, some reference ages are reported on the basis of dating performed by Schwander and others (2001). The Antarctic Cold Reversal (ACR) oscillation considered here is the period included between the ACR onset as reported by Jouzel and others (2001) (around 14 kyr BP) and the end of transition (11.6 kyr BP).

Both profiles show a marked concentration decrease in the last glacial/interglacial transition, from mean values of 0.4 and 1.5 µg L^{-1} in the glacial, to 0.08 and 0.09 µg L^{-1} in the Holocene for Fe and Al respectively. The concentration variability, expressed by the bag standard deviation, also shows a drop in the absolute value from the Late-glacial to the interglacial period (see vertical bars in the plot). The decreasing concentration trend is consistent with the ionic components and dust mass pattern measured along ice core EDC96 (Delmonte and others, 2002; Röthlisberger and others, 2002; Traversi and others, 2002).

Fe and Al exhibit a different behaviour during the ACR. Fe shows sensitivity to the ACR oscillation, when the highest values are close to those of the glacial period, and also shows a higher relative standard deviation (105% in the ACR and 60% in the glacial).

Aluminium sensitivity to the ACR is less evident, instead showing concentrations and relative standard deviations similar to Holocene levels, so that the Al CFA profile is similar to the dust mass profile along the EDC96 ice core (Delmonte and others, 2002).

As discussed above, Al and Fe determined by CFA are representative of the available (free or weakly complexed) fraction after filtration on 5.0 µm and acidification to pH 2.0. A comparison with the Al and Fe content, as measured by
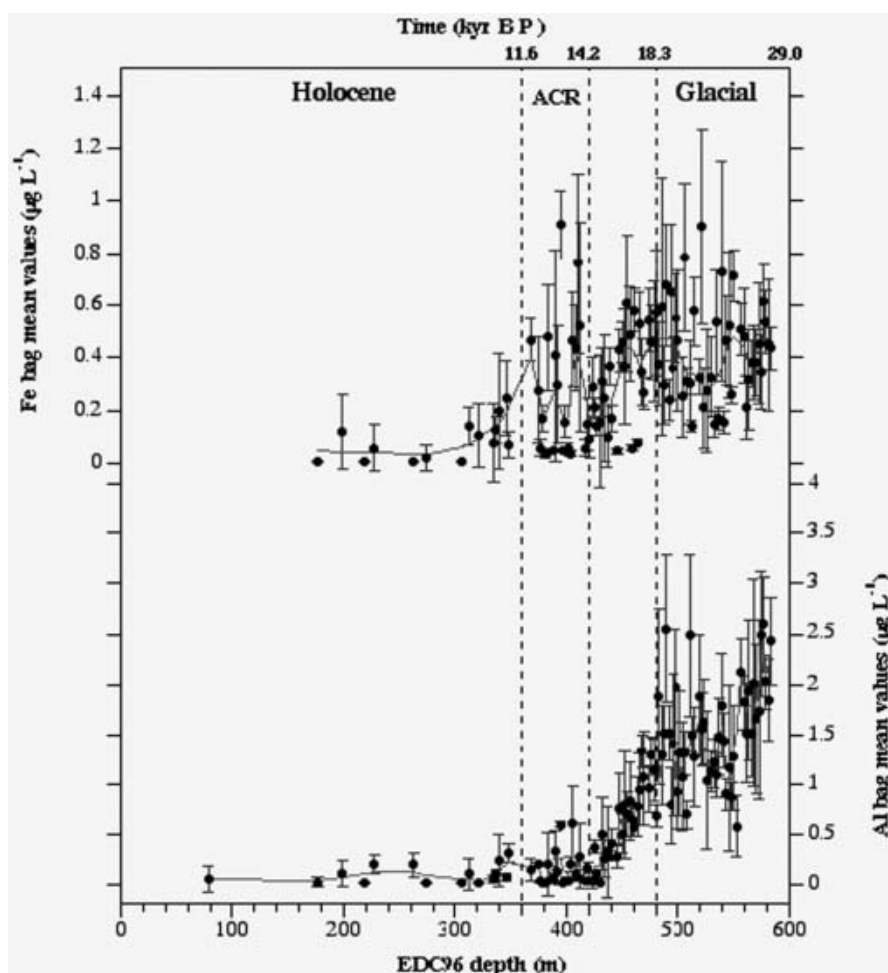
Fig. 3. Concentration vs depth profile for Fe and Al in the EDC96 ice core. Dots indicate the bag average values (each bag is 55 cm long), and the vertical bars indicate the bag standard deviation. The bold lines represent the 10% (Fe) and 5% (Al) weighted fitting curves. The depth range labelled as ACR in the plot actually refers to the total isotopic oscillation: from ACR onset to the end of the transition.

ICP-SFMS, was carried out in order to evaluate the percentage of metal which CFA methods are able to measure.

Figure 4 shows mean Fe and Al contents determined by CFA and ICP-SFMS in the different climatic periods. Each plot also reports the absolute standard deviation associated with mean values.

Mean Fe and Al values measured by ICP-SFMS also present a decreasing trend from the high levels recovered in the glacial period (13.4 and 13.8 $\mu g\,L^{-1}$ for Fe and Al, respectively) to lower levels in the Holocene (0.24 and 0.47 $\mu g\,L^{-1}$ for Fe and Al, respectively), with a similar decrease in absolute standard deviation. The relative standard deviation for Al ranges between 53% (Holocene) and 81% (glacial), while a higher variability is shown by Fe in the ACR (167%) with respect to Holocene and glacial (97% and 86%, respectively).

The percentage of Fe content determined by CFA with respect to Fe content determined by ICP-SFMS differs greatly in the three periods, with a minimum in the glacial period (3%), a maximum in the ACR (64%) and an intermediate value in the Holocene (34%). This pattern is explained by the different availability of Fe in the three climatic periods, probably in relation to a different size distribution and/or different chemical species characterizing the associated aerosol particles. As for Fe, besides the known primary crustal source, a 'secondary crustal source' can be

hypothesized, related to biogenic marine recycling of dust deposition containing Fe. Iron arising from the latter source is likely to be present in marine aerosol in a more available form with respect to the direct crustal source. Crustal sources of Fe are likely to dominate in the glacial period, with enhanced concentration values with respect to the Holocene, leading to low available-Fe contents and low Fe CFA/ICP-SFMS percentages.

The sharp increase in such percentages in the ACR suggests that transport processes delivering marine air masses (along with more soluble Fe species) to the Dome C site are enhanced, as shown by the high sensitivity of the typical sea-spray markers (Na^+ and Mg^{2+}) in this climatic period (Traversi and others, 2003; Udisti and others, 2004).

By contrast, Al CFA/ICP-SFMS show a lower variability in the three climatic periods, ranging from 11% in the glacial to 25% during the ACR oscillation, demonstrating that the available Al fraction is less sensitive to climatic and environmental variations. Aluminium CFA content appears to be mainly controlled by crustal sources and can be considered a crustal proxy marker for evaluating the relative contribution of extra-crustal iron.

Figure 5 reports the Fe/Al ratio, where both elements were determined by CFA, as a function of depth. Since Fe and Al measured by CFA represents only a fraction of the total content, the theoretical Fe/Al crustal ratio (0.677 w/w;
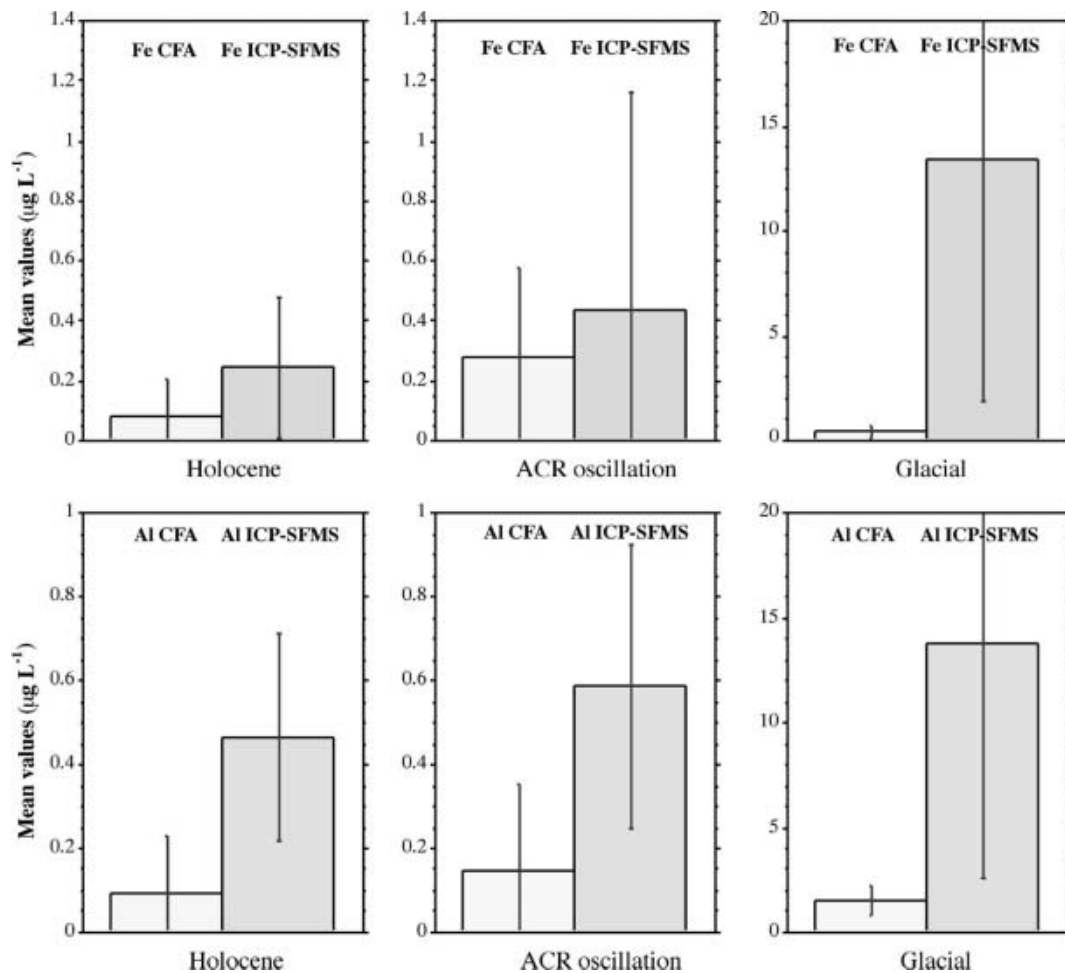
Fig. 4. Comparison between mean Fe and Al values determined by CFA and ICP-SFMS in the three considered climatic periods (Holocene, ACR oscillation, glacial period). The vertical bars represent the related absolute standard deviation. Notice that the concentration scale for the glacial period is much larger than those for the Holocene and ACR.

Weast, 1987–88) was corrected on the basis of the average percentage of each metal (3% and 11% for Fe and Al, respectively) measured in the glacial period, assuming that ICP-MS determinations reflect the total budget and that the crustal component is dominant for both metals in this period. The calculated Fe/Al available crustal ratio (0.185 w/ w) is indicated by the horizontal line in Figure 5. Fe/Al ratios measured in samples from the glacial period fall near the calculated Fe/Al available crustal ratio. In the 560–585 m depth range, where there is a maximum in the Ca^{2+} depositional flux (Röthlisberger and others, 2002; Udisti and others, 2004) in relation to dust content, there is a low dispersion of data and the Fe/Al ratio falls on the reference line. Moving towards the ACR, the Fe/Al CFA ratio sharply increases until it reaches values about two orders of magnitude higher than the estimated crustal ratio. In the Holocene, the Fe/Al ratio gradually decreases, and values generally fall above the crustal reference line. This behaviour confirms the importance of Fe extra-crustal sources in the ACR, which also play a significant role in the Holocene.

CONCLUSIONS

Aluminium and iron are considered typical markers of primary atmospheric aerosol of crustal origin. This source

can be considered dominant for aluminium; for iron, the metabolic processes in which it takes part as an essential oligo-element must also be taken into account. Deposition of iron-containing dust arising from desert regions over oceanic areas was shown to be a growth factor for phytoplanktonic species. Therefore, iron content in aerosol during glacial/interglacial transitions is believed to play a relevant role in controlling oceanic phytoplankton uptake of atmospheric CO_2.

Aluminium and iron concentrations recorded in ice sheets can provide detailed, high-temporal-resolution data on global climatic and environmental changes.

The two CFA methods presented can be used to determine available Fe and Al fractions in the EPICA Dome C ice core from the last 28 kyr. Both elements show high values in the Last Glacial Maximum (LGM) but are characterized by a different decreasing trend during the transition, reaching low values in the Holocene. Both components allow identification of the ACR oscillation, although Fe is highly sensitive to this climatic change, reaching values similar to those determined in the LGM.

A comparison with Fe and Al ICP-SFMS measurements, believed to represent the total metal content, revealed that the CFA-Fe percentage, unlike the CFA-Al percentage, was highest in the ACR and lowest in the LGM.

A possible explanation for these results is that the
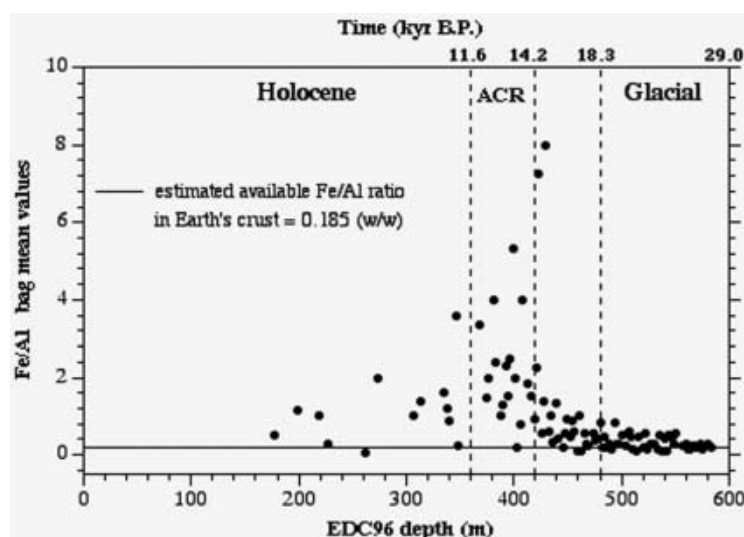
Fig. 5. CFA Fe/Al ratio as function of depth. The depth range labelled as ACR in the plot actually refers to the total isotopic oscillation: from ACR onset to the end of the transition. The horizontal line indicates the estimated available Fe/Al ratio in Earth's crust (see text for details).

dominant Fe input during the LGM arises from insoluble continental dust, while the prevailing Fe chemical form in the ACR is soluble and more available for CFA measurement, suggesting that oceanic-recycled Fe, mainly distributed as fine particles and as more soluble species, plays a relevant role in the latter period.

Further measurements with higher temporal resolution are needed to confirm the observed behaviour.

REFERENCES

Andreae, M. O. 1996. Raising dust in the greenhouse. *Nature,* **380**(6573), 389–390.

Barbante, C. *and 9 others*. 1997. Direct determination of heavy metals at picogram per gram level in Greenland and Antarctic snow by double focusing inductively coupled plasma mass spectrometry. *J. Analy. Atomic Spectrom.,* **12**(9), 925–931.

Barbante, C. *and 6 others*. 1999. Trace element determination in alpine snow and ice by double focusing inductively coupled plasma mass spectrometry with microconcentric nebulisation. *J. Analy. Atomic Spectrom.,* **14**(9), 1433–1438.

Chereskin, B. M. and P. A. Castelfranco. 1982. Effects of ion and oxygen on chlorophyll biosynthesis. *Plant Physiology,* **68**, 112–116.

De Angelis, M., M. Legrand, J.-R. Petit, N. I. Barkov, Ye. S. Korotkevich and V. M. Kotlyakov. 1984. Soluble and insoluble impurities along the 950 m deep Vostok ice core (Antarctica) – climatic implications. *J. Atmos. Chem.,* **1**, 215–239.

De Angelis, M., N. I. Barkov and V. N. Petrov. 1987. Aerosol concentrations over the last climatic cycle (160 kyr) from an Antarctic ice core. *Nature,* **325**(6102), 318–321.

Delmonte, B., J.-R. Petit and V. Maggi. 2002. Glacial to Holocene implications of the new 27000-year dust record from the EPICA Dome C (East Antarctica) ice core. *Climate Dyn.,* **18**(8), 647–660. (10.1007/s00382-001-0193-9.)

Duce, R. A. 1995. Sources, distributions and fluxes of mineral aerosols and their relationship to climate. *In* Charlson, R. J. and J. Heitzenberg, *eds. Dahlem Workshop on Aerosol Forcing of Climate, April 24–29, Berlin.* Chichester, John Wiley and Sons, 43–72.

Finden, D. A. S., E. Tipping, G. H. M. Jaworski and C. S. Reynolds. 1984. Light-induced reduction of natural iron (III) oxide and its relevance to phytoplankton. *Nature,* **309**(5971), 783–784.

Greene, R. M., Z. Kolber, D. G. Swift, N. W. Tindale and P. G. Falkowski. 1994. Physiological limitation of phytoplankton photosynthesis in the eastern equatorial Pacific determined from variability in the quantum yield of fluorescence. *Limnol. Oceanogr.,* **39**(5), 1061–1074.

Hirayama, K. and N. Unohara. 1988. Spectrophotometric catalytic determination of an ultratrace amount of iron (III) in water based on the oxidation of N,N-dimethyl-p-phenylendiamine by hydrogen peroxide. *Anal. Chem.,* **60**(23), 2573–2577.

Johnson, K. S., R. M. Gordon and K. H. Coale. 1997. What controls dissolved iron concentrations in the world ocean? *Mar. Chem.,* **57**(3–4), 137–161.

Jouzel, J. *and 12 others*. 2001. A new 27 kyr high resolution East Antarctic climate record. *Geophys. Res. Lett.,* **28**(16), 3199–3202.

Legrand, M. R., C. Lorius, N. I. Barkov and V. N. Petrov. 1988. Vostok (Antarctica) ice core: atmospheric chemistry changes over the last climatic cycle (160,000 years). *Atmos. Environ.,* **22**(2), 317–331.

Mánuel-Vez, M. P., C. Moreno, D. J. González and M. García-Vargas. 1997. Direct fluorometric determination of dissolved aluminium in seawater at nanomolars level. *Anal. Chim. Acta,* **355**(2–3), 157–161.

Martin, J. H. 1990. Glacial–interglacial CO_2 change: the iron hypothesis. *Paleoceanography,* **5**(1), 1–13.

Martin, J. H. and S. E. Fitzwater. 1988. Iron deficiency limits phytoplankton growth in the north-east Pacific subarctic. *Nature,* **331**(6154), 341–343.

Measures, C. I. 1999. The role of entrained sediments in sea ice in the distribution of aluminium and iron in the surface waters of the Arctic Ocean. *Mar. Chem.,* **68**(1–2), 59–70.

Measures, C. I., J. Yuan and J. A. Resing. 1995. Determination of iron in seawater by flow injection analysis using in-line preconcentration and spectrophotometric detection. *Mar. Chem.,* **50**(1–4), 3–12.

Nishikawa, Y., K. Hiraki, K. Morishige and T. Shigematsu. 1967. [Fluorometric determination of aluminium and gallium with lumogallion.] [In *Japan Analyst,* **16**, 692–697. Japanese.]

Planchon, F. A. M. *and 7 others.* 2001. Ultrasensitive determination of heavy metals at the sub-picogram per gram level in ultra-clean Antarctic snow samples by inductively coupled plasma sector field mass spectrometry. *Anal. Chim. Acta,* **450**(1–2), 193–205.

Prospero, J. M. 1996. The atmospheric transport of particles to the ocean. *In* Ittekkot, V., S. Honjo and P. J. Depetris, *eds. Particle flux in the ocean.* Chichester, etc., John Wiley and Sons Ltd, 19–52. (SCOPE Report 57.)

Raven, J. A. 1990. Predictions of Mn and Fe use efficiencies of phototrophic growth as a function of light availability for growth and of C assimilation pathway. *New Phytol.,* **116**(1), 1–18.

Resing, J. A. and C. I. Measures. 1994. Fluorometric determination of Al in seawater by flow injection analysis with in-line preconcentration. *Anal. Chem.,* **66**(22), 4105–4111.

Röthlisberger, R. *and 6 others.* 2000. Technique for continuous high-resolution analysis of trace substances in firn and ice cores. *Environ. Sci. Technol.,* **34**(2), 338–342.

Röthlisberger, R. *and 6 others.* 2002. Dust and sea salt variability in central East Antarctica (Dome C) over the last 45 kyrs and its implications for southern high-latitude climate. *Geophys. Res. Lett.,* **29**(20), 1963. (10.1029/2002GL015186.)

Schwander, J., J. Jouzel, C. U. Hammer, J. R. Petit, R. Udisti and E. Wolff. 2001. A tentative chronology for the EPICA Dome Concordia ice core. *Geophys. Res. Lett.,* **28**(22), 4243–4246.

Sutheimer, S. H. and S. E. Cabaniss. 1995. Determination of trace aluminum in natural waters by flow-injection analysis with fluorescent detection of the lumogallion complex. *Anal. Chim. Acta,* **303**(2–3), 211–221.

Sutheimer, S. H. and S. E. Cabaniss. 1997. Aluminum binding to humic substances determined by high performance cation exchange chromotography. *Geochim. Cosmochim. Acta,* **61**(1), 1–9.

Traversi, R., S. Becagli, E. Castellano, A. Migliori, M. Severi and R. Udisti. 2002. High-resolution fast ion chromatography (FIC) measurements of chloride, nitrate and sulphate along the EPICA Dome C ice core. *Ann. Glaciol.,* **35**, 291–298.

Traversi, R., S. Becagli, S. Benassai, E. Castellano, I. Fattori and R. Udisti. 2003. Sea-salt components behaviour in the last glacial/interglacial transition from the analysis of the EDC96 ice core. *Terra Antartica Reports,* **8**, 101–105.

Udisti, R. *and 9 others.* 2004. Sensitivity of chemical species to climatic changes in the last 45 kyr as revealed by high-resolution Dome C (Antarctica) ice-core analysis. *Ann. Glaciol.* **39** (see paper in this volume).

Weast, R. C., *ed.* 1987–88. *CRC handbook of chemistry and physics. Sixty-eighth edition.* Boca Raton, FL, CRC Press.

Wells, M. L., L. M. Mayer, O. F. X. Donard, M. M. de Souza Sierra and S. G. Ackelson. 1991. The photolysis of colloidal iron in the oceans. *Nature,* **353**(6341), 248–250.